Energy absorption analysis of density graded aluminum foam

Li, Jingde; Ma, Guowei; Zhou, Hongyuan; Du, Xiuli

2011

Li, J., Ma, G., Zhou, H., & Du, X. (2011). Energy Absorption Analysis of Density Graded Aluminium Foam. International Journal of Protective Structures, 2(3), 333-350.

https://hdl.handle.net/10356/94970

https://doi.org/10.1260/2041-4196.2.3.333

Energy Absorption Analysis of Density Graded Aluminium Foam

Jingde Li[1,a], Guowei Ma[1,b], Hongyuan Zhou[2,c] and Xiuli Du[3,d]
[1]School of Civil and Resource Engineering, The University of Western Australia, 35, Stirling Highway, Crawley WA 6009, Australia
[2]School of Civil and Environmental Engineering, Nanyang Technological University,
50 Nanyang Avenue, 639798,Singapore
[3]College of Arthitecture and Civil Engineering, Beijing University of Technology, Beijing, China
[a]jaden_li@hotmail.com, [b]ma@civil.uwa.edu.au,
[c]zhou0107@e.ntu.edu.sg, [d]Duxiuli@bjut.edu.cn

ABSTRACT
A numerical approach is carried out to investigate the energy absorption efficiency of density graded aluminium foam. Effects of blast load impact velocity, loading duration and sample thickness on the input energy density and output energy density of the graded foam are investigated. The stochastic meso-scale aluminium foam structure is generated by adopting a 2D Voronoi technique and the commercial software ANSYS/LS-DYNA is used for the FE modelling. Parametric study shows that the density graded aluminium foam is effective in improving energy absorption capability while keeping a lower stress transmitted to the substrate or the protected structure if it is properly designed.

Keywords: Energy absorption, Density graded foam, Voronoi structure, Numerical analysis, Blast mitigation.

1. INTRODUCTION

Structural retrofit using a novel energy-absorption sacrificial metallic foam cladding has become a preferable and economical approach for structure protection against blast loads and it is of great interest for aeronautical design, marine and defence industries [1]. As a stratified complex structure, the metallic foam cladding is usually composed of two dense stiff buffer plates and a central core of cellular metal that endows them with not only high specific strength and modulus, but also relatively low density and surpassing energy absorption capacity to undergo large deformation while sustaining the nearly constant stress value.

There have been numerous theoretical, experimental and numerical investigations conducted on open-cell and closed-cell foamed metals. Some aspects of the behaviour of cellular solids have been systematically introduced by Gibson and Ashby [2] as well as Ashby *et al*. [3]. Shu and Goh [4] assessed the Young's modulus of foam structure by using

the cubic cell model as well as Andrews' [5] analytical research on uniaxial compressive and tensile behaviour of several aluminium foams. Paul and Ramamurty [6] experimentally investigated the strain rate sensitivity of closed cell aluminium foam (ALPORAS) in agreement with the conclusion of Wang *et al*. [7] and Mukai *et al*. [8] that the plateau stress of the metallic foam is highly sensitive to the high strain rate within and over a certain range, while the opposite standpoint was given by Ruan *et al*. [9] who performed the experimental test on compressive behaviour of CYMAT aluminium foams with various relative densities at different strain rates and found that the nominal stress was insensitive to the strain rate. In terms of numerical investigations, Overaker *et al*. [10] applied a two-dimensional model studying the elastic behaviour of regular hexagonal foams, both convex and non-convex. Silva *et al*. [11] analysed the influence of non-periodic microstructure and missing cell walls on the elastic modulus of compressive failure behaviour of 2D Voronoi honeycombs using finite element analysis. Zheng *et al*. [12] found that increasing the cell irregularity led to an increase in the plateau stress, thereby improving the energy absorption capacity. Papka and Kyriakides [13] simulated the crushing process of full-scale FE honeycomb models using ABAQUS, which reproduced the experimental results qualitatively and quantitatively. Zhu *et al*. [14] proposed a numerical study on square metallic sandwich panels subjected to air blast loading, which provided an insight into the deformation mechanism of the panels under blast load and the FE simulation results demonstrated a good agreement with the data obtained from experimental tests.

The aim of the current work is to simulate and discuss the energy absorbing characteristics of graded aluminium foams based on the prior research conducted on the homogeneous foams. The graded cellular materials with non-uniform porosity are frequently seen in nature, for instance, bones and woods. An example is illustrated by Daxner [15] that the regions of dense "cortical" bone has neighbour regions of lower-density "trabecular" bone so that the density of bone is distributed in space to optimise the overall performance. Ajdari *et al*. [16] simulated two-dimensional graded Voronoi structures with finite element method to explore the elastic-plastic mechanical properties, such as the effective elastic modulus and the yield strength under both uni-axial and bi-axial compression and the sensitivities to density gradient. Lee *et al*. [17] adopted a micromechanical method to predict the fracture toughness to understand the fracture behaviour, which indicated that the fracture toughness of functionally graded foam material mainly depends on the relative density at the crack-tip. Meguid *et al*. [18] modelled the localization of deformation in cellular materials due to the spatial density variations and material defects. It was found that the localization pattern and the compressive stress versus nominal strain curve were in good agreement with experiments only if the appropriate density distribution is taken into account. However, the dynamic responses and energy absorption efficiency of graded foams remain debatable and needs further exploration.

In the present study, numerical simulations by employing a meso-scale Voronoi tessellation model are conducted to analyse the energy absorbing ability and effectiveness of aluminium foam with graded densities. The density graded aluminium foam is sandwiched between a moving rigid wall and a stationary wall, while the blast load is applied on the moving wall so that the deformation occurs from one side towards the other; the nominal compressive stress-strain curves in regard to the energy density or energy per unit volume are achieved at both the impact and the stationary sides. Three layers of aluminium foams with different relative densities are considered. The numerically simulated uniaxial stress-strain relationship of individual relative density foam is calibrated by comparing to the experimental results. Energy absorption efficiency of the graded foam cladding is then

investigated and compared to those of homogeneous foams. Parametric study concerning effects of blast load impact velocity, loading duration and sample thickness is subsequently performed.

2. VORONOI DIAGRAM GENERATION

The construction of meso-scale numerical model is first carried out. The two-dimensional Voronoi tessellation is generated by using a Matlab program to form the nucleation and growth of cells. Nucleation points are generated in the square area A_0 of size $L \times L$ by creating the x and y coordinate independently from random numbers distributed between zero and one. Each subsequent stochastic point is accepted provided that it is greater than a minimum allowable distance δ between any two nuclei, until n nuclei are seeded in the square [19].

To construct a regular 2D Voronoi diagram with n cells in the area A_0, the distance d_0 between any two neighbouring nucleation points should be constant and given by

$$d_0 = \sqrt{\frac{2A_0}{3^{1/2}n}} \tag{1}$$

A parameter α is defined to measure the regularity of the 2D Voronoi structure:

$$\alpha = \frac{\delta}{d_0} \tag{2}$$

The nuclei will be distributed entirely at random in space following the Poisson distribution, provided that the value of α equals to zero. Figure 1 presents samples of a regular honeycomb with regularity, i.e., $\alpha = 1$ ($\delta = d_0$) and a random tessellation with the magnitude of regularity, i.e., $\alpha = 0$. The effect of the irregularity α has been studied by Luxner *et al*. [20]. Obviously, the irregularity has an important influence on both the static and dynamic mechanical properties of porous metallic foams. The focus of the present study is on the dynamic effect of the cellular material with the same irregularity, i.e. α is fixed as 0.7.

The relative density of Voronoi foams is defined as:

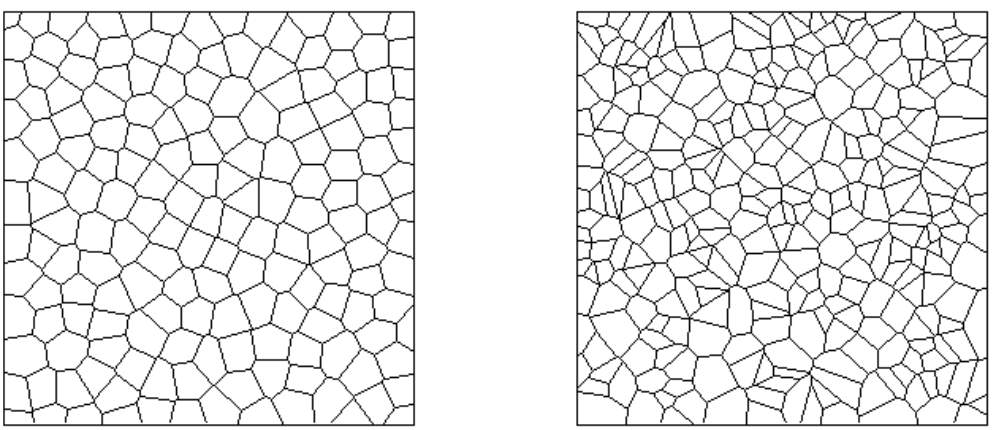

α=1 α=0

Figure 1: Voronoi diagrams with different regularities.

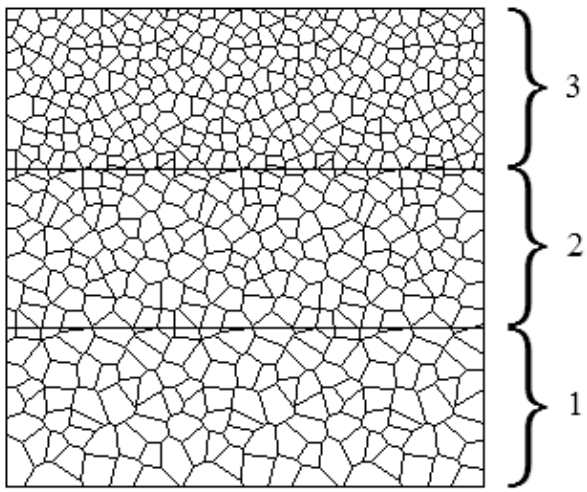

Figure 2: Density graded Voronoi foam.

$$\frac{\rho^*}{\rho_s} = \frac{\sum l_i \cdot t_i}{L^2} \tag{3}$$

where ρ^* and ρ_s refer to densities of the cellular and solid materials respectively, t_i and l_i are the thickness and length of cell walls, L is the sample length of the square area A_0. The Voronoi foam is then separated into three equal parts ($\Delta y = L/3$) as shown in Figure 2. The density gradient for parts k and $k + 1$ (for $k = 1,2$) is specified as

$$\nabla_\rho = \frac{\rho^*_{k+1} - \rho^*_K}{\rho^*_{K+1}} = \frac{\left(\sum l_i t_i\right)_{k+1} - \left(\sum l_i t_i\right)_k}{\left(\sum l_i t_i\right)_{k+1}} \tag{4}$$

To develop the 3D cellular configuration in the numerical simulation by using finite element software ANSYS/LS-DYNA, the Voronoi tessellation is extruded along the out-

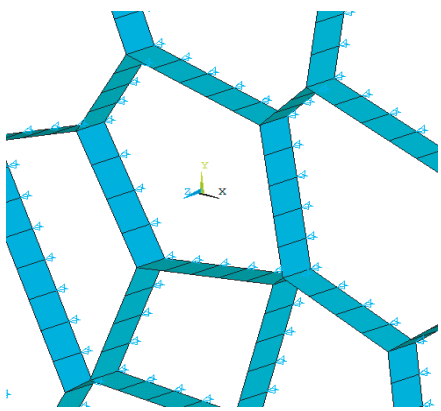

Figure 3: 3-D shell elements.

of-plane direction (z-axis) so that there is only one segment when the cell walls are discretized by choosing shell elements with the average length of 0.5 mm, as seen in Figure 3. Large displacement and nonlinear analysis have been considered by ANSYS/LS-DYNA. The movement of foam along z-axis is restricted and all the nodes at the stationary side are constrained, whereas the moving side is allowed to slip along the rigid wall. Automatic single surface contact is employed to all cell walls to enable simulation of the contacts between different cells in the crushing process. A nonlinear elastic-plastic model with isotropic hardening and von Mises yield criterion is adopted for the shell elements.

In the present study, the relative density is controlled by changing the numbers of cell walls in the sample according to an assigned foam density while the thickness of cell walls in each part is kept constant. Three homogenous foam samples with different relative densities are initially generated in the FE modelling to calibrate the numerical results with experimental tests, which will be discussed in the following section. The density graded foam with the decreasing gradient of 20% is developed by combining those three tailored foam layers into an ensemble, as shown in Figure 2. It is worth noting that the junctures of cell walls between different layers are automatically generated in the Matlab program.

3. CALIBRATION OF THE NUMERICAL MODEL

A comprehensive experimental program, which had been undertaken by Ruan *et al*. [9] on the dynamic compressive behaviour of CYMAT aluminium foams at low and medium strain rates, is chosen as the benchmark in the calibration of the numerical model. The CYMAT materials in the experiments were made of aluminium with a Young's modulus of 93 GPa and upper yield compressive strength of 310 MPa. The cell sizes of foams changed with their densities. The lower the density, the larger is the cell size. Six different dimensions of the samples were varied from 50×50×25 mm to 150×150×50 mm as well as the relative densities in the region of 5%–20% were employed in order to cover a sufficient number of cells. There were two thin layers of aluminium plate on two opposite surfaces in the thickness direction, which was also the crushing direction. A material test system (MTS) machine was utilized to perform the compressive tests at strain rates of $10^{-3} - 10^{+1}\ s^{-1}$ to these closed cell aluminium foams. The stress-strain curves were analysed when the samples subjected to the load lead the top ram moved downward at a constant velocity whilst the bottom ram of the machine was kept motionless. The numerical simulation followed exactly the same process.

In order to calibrate the meso-scale Voronoi models, numerical simulations of the physical tests done by Ruan *et al*. [9] are performed by using ANSYS/LS-DYNA for samples of the size 50 mm×50 mm with relative densities of 11.1%, 14.8% and 18% respectively. The solid aluminium density, Young's modulus, yield stress, Poisson's ratio, tangent modulus, friction coefficient at contact are 2.7×10^3 kg/m^3, 93 GPa, 210 MPa, 0.3, 4 GPa, and 0.2 respectively. The impact rigid wall is loaded at a low velocity impact of 0.5 m/s. The reaction forces are divided by the contact areas both at the impact and the stationary sides of the rigid walls to determine the crushing stresses, and the nominal strain is calculated as the compressive deformation of the sample over the sample height L. In order to reduce the total computational time, the so-called 'mass scaling approach' is employed to control the minimum time step size Δt and the element density is adjusted to achieve a specified time step size:

$$\nabla t_{specified} = \sqrt{\frac{\rho_i \cdot l_{ei}^2 \cdot \left(1 - v^2\right)}{E}} \quad \text{in element } i \tag{5}$$

Table 1: Comparison of plateaus stresses between experiments and simulations

Experimental Relative density	Numerical Relative density	Experimental σ_{cn} (MPa)	Numerical σ_{cn} (MPa)	Error of σ_{cn} (MPa)
10.44%	11.1%	1.508	1.234	18.16%
14.08%	14.8%	4.244	3.979	6.248%
17.68%	18%	8.069	7.345	8.973%

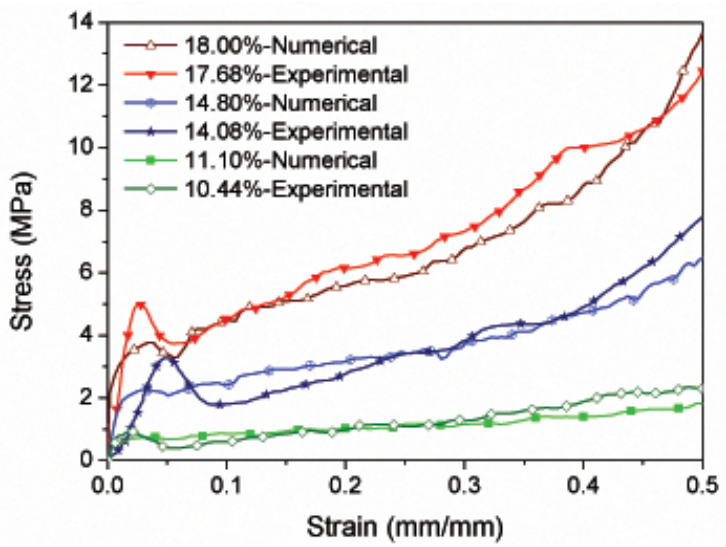

Figure 4: Comparison of stress-strain curve between experimental and numerical results.

where l_{ei} is the element size, v, E and ρ_i are the Poisson's ratio, the Young's modulus and the specific mass density.

Table 1 and Figure 4 are the comparisons of experimental and FE simulation results. The contrastive nominal stress σ_{cn} is defined as the mean stress over a strain range of 0.1–0.5 to obtain a quantitative relation between the relative densities in the comparisons.

It can be seen from Figure 4 that the correlation between the experiment tests and FE simulations is satisfactory; though the errors of contrastive nominal stresses vary with disparate relative densities. Firstly, it can be explained that there is a slight difference of relative density between the experimental test and numerical simulation in each comparison, due to the fact that the value of relative density in numerical modelling is approximately determined by generating different numbers of cells in the foam after several trials. Secondly, the size effect is not considered and the impact velocity in the numerical simulations is kept to be constant at 0.5 m/s (i.e., strain rate $\dot{\varepsilon} = 10^{+1}s^{-1}$), while the laboratory programs of Ruan *et al*. [9] were performed in the strain rate region of $10^{-3} - 10^{+1}$ s^{-1} based on the conclusion that the nominal stress at plateau is insensitive to the strain rate within this range. The slight discrepancies of plateau stresses in each experimental test group existed when the strain rates varied from 10^{-3} s^{-1} to $10+^{1}$ s^{-1}.

4. ENERGY ABSORPTION OF HOMOGENOUS FOAM

In terms of the energy absorption, the FE simulations are performed on homogenous foams by applying the same loading condition as it is employed in calibration, namely the constant impact velocity is 0.5 m/s. The energy density or volumetric energy absorption (W) is defined as the energy absorption per unit volume for the foam samples which is calculated to be the area under the stress-strain curve, as shown in Figure 4 (i.e., $W = \sigma_0 \cdot \varepsilon_D$). For uniform density foams, the densification strain ε_D and the foam plateau stress σ_0 can be defined as [21]:

$$\varepsilon_D = 1 - \lambda \cdot \rho^* / \rho_s \tag{6}$$

$$\sigma_0 = \frac{1}{\varepsilon_D} \int_0^{\varepsilon_D} \sigma d\varepsilon \tag{7}$$

where λ is taken as 3.0 in this study.

The results of the simulations for each segment in Table 2 indicate that the energy absorption capacity is sensitive to its relative density ρ^*/ρ_s. The nominal stress of the aluminous Voronoi foam increases with the relative density, whereas the densification strain ε_D slightly declines. In terms of the performance of energy absorption, it is clear that this structure possesses the best energy absorption capacity when the foam core density rises to 486 kg/m^3 or 18% of relative density. However, due to the higher crushing stress, the force transferred to the protected structure by the foam with relative density of 18% will also be the highest.

Table 2: Relative density effect

Sample No.	Relative density ρ^*/ρ_s (%)	σ_0 (MPa)	ε_D (mm/mm)	Volumetric energy absorption W (MJ/m^3)
1	11.1	1.480	0.667	0.987
2	14.8	4.626	0.556	2.572
3	18	6.740	0.460	3.100

5. ENERGY ABSORPTION OF DENSITY GRADED FOAM

In order to protect the structure behind the sacrificed foam cladding, not only should the high energy be absorbed efficiently but the transferred stress should be kept low enough to not cause the damage, thus the density graded foam is introduced in the following discussion.

It should be mentioned that it has been verified that the foamed material will fail under different modes with respect to different impact velocities [22, 23]. Under a high velocity impact, the homogeneous foam material undergoes a progressive failure mode, and the foam is crushed progressively from the impact side, and a low velocity impact will result in a random failure mode which deforms mainly due to the weaker links. A moderate impact velocity leads to a combined failure mode of the above two. Obviously the failure modes highly rely on the impact velocity and the relative density of the foam material. On the other hand, a progressive failure mode exhibits higher energy absorption capacity and a lower relative density foam may transfer smaller forces to the protected structure. Thus it is possible that a density graded foam will behave more excellently than a homogeneous foam in terms of absorbing more energy while transferring a lower force to the protected structure when it is subjected to a blast load. To verify this concept, three different relative density

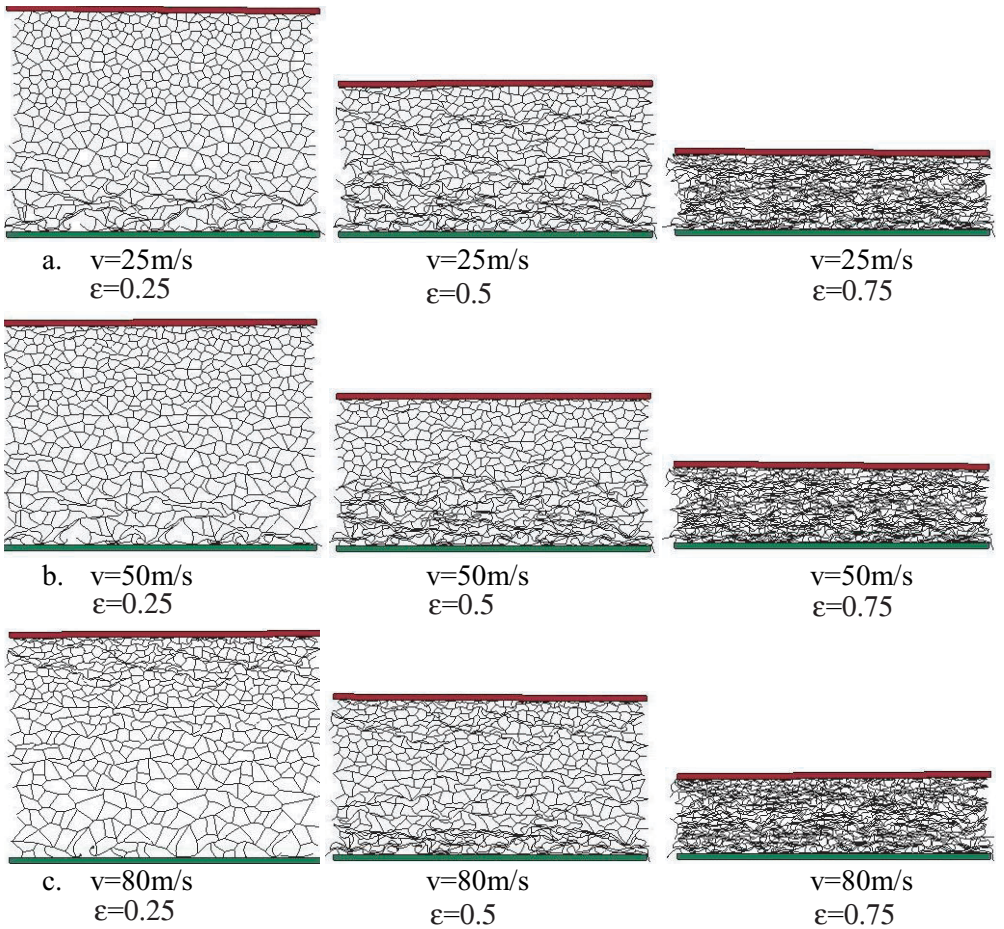

Figure 5: Failure mode under various impact velocities.

foams with thickness of L/3 are stacked together, i.e. density 1 of 11.1%, density 2 of 14.8% and density 3 of 18%, to form the density graded structure. The simulations of density graded structures subjected to different impact velocities (i.e. 25 m/s, 50 m/s, 80 m/s) are carried out to catalogue the deformation modes as shown in Figure 5.

It is noted that at a lower impact velocity (25 m/s), deformation firstly occurs at the bottom soft layer during a very short time to absorb energy, whereas the top and base of foam material collapses simultaneously under moderate velocity (50 m/s), which absorbs more energy with further densification and the peak stress can be found at the hardest layer. As to the adequately high impact velocity (80 m/s), the structure deforms progressively from the impact side, which maximizes the energy absorption by the densest part, and the graded foam is fully densified along the compressive direction to the stationary side. The weakest layer is crushed at the last so that the compressive stress declines to the smallest magnitude.

Therefore, it is believed that the density graded structure performs better when it is subjected to a higher impact velocity. For simplicity, a triangular blast load is applied with a peak impact velocity of 80 m/s and a duration of 0.3 ms. The simplification of blast load is also utilized in the parametric study which will be carried out in the following section.

Also, it has been proved that the stress time history at the impact side is different from

that at the stationary side due to inertia effect (Ma and Ye [23]). Different from a quasi-static case, two different energy densities are defined. The input energy density is calculated based on the stress time history at the impact side while the output energy density is calculated based on that at the stationary side. The nominal strain is remained to be determined according to the total compaction over the total thickness of the foam sample. It is obvious that the input energy density is related to the energy absorption capacity of the foam sample, while the output energy density represents the residual energy. An energy absorption efficiency factor is defined as

$$e = \frac{W_{input} - W_{output}}{W_{input}} \times 100\% \tag{8}$$

where W_{input} and W_{output} are the input energy density or the absorbed energy per volume and the output energy density or the residual energy per volume respectively. For comparison reason, the two energy densities are integrated from the area under the nominal stress-strain

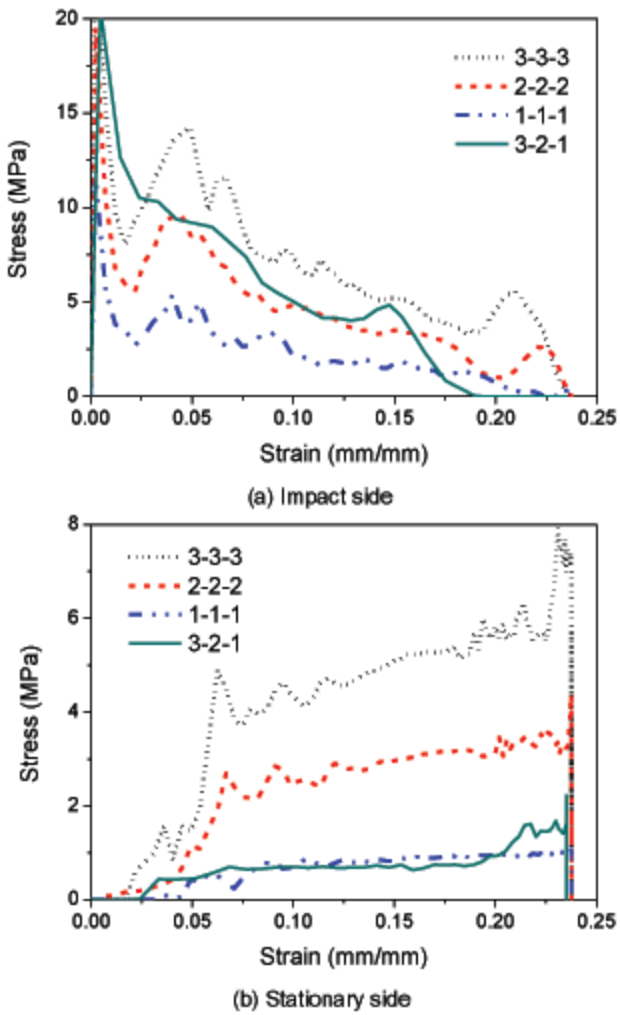

Figure 6: Compressive stress vs. nominal strain of foam core composition.

Table 3 Relative density effect

Foam core composition	Foam core density (kg/m^3)	Winput (MJ/m^3)	Woutput (MJ/m^3)	σ_0 (MPa)	Energy absorption efficiency factor
1-1-1	300	0.5524	0.1517	0.639	72.54%
2-2-2	400	1.1233	0.5421	2.282	51.74%
3-3-3	486	1.7287	0.9588	4.037	44.54%
3-2-1	395.3	1.2782	0.1625	0.685	87.29%

[a] σ_0 is the average stress over the strain range corresponding to Eqn.(9)
[b] 1,2,3 denote the relative density of 11.1%, 14.8% and 18%.

curves up to a strain level, which is defined as 0.5 in the present study.

The comparisons of stress-strain curves at the impact side and the stationary side are shown in Figure 6. It is clearly seen that stress-strain curves at the impact and stationary sides are different and thus so are the input and output energy densities. Table 3 lists the input and output energy densities and the efficiency factor of different foam density combinations. It is seen that the graded aluminium foam composed of 3 layers (i.e. relative densities of 11.1%, 14.8%, and 18%) absorbs the energy 56.78% higher than that of the homogenous foam 1-1-1 with 11.1% relative density at the impact side but nearly as the same value of plateau stress at the stationary side. On the other hand, the transferred stress on the protected structure of graded material is significantly lower than that of uniform foam of 14.8% relative density, but it possesses slightly greater energy absorption capacity at the impact side. The energy absorption efficiency factor reduces with the relative density of homogenous foams, whilst the graded one gives the largest efficiency factor, i.e., 87.29%.

Therefore, it is obvious that the density graded structure behaves better than those homogenous foams subjected to dynamic loading. Specifically, the density graded foam can efficiently absorb the energy and transmit the stress to a desirable low value to protect the structure behind the sacrificial material.

6. PARAMETRIC STUDY

Having validated the numerical simulation results by experimental tests as well as the novel mechanical properties of graded aluminium foam under high velocity discussed above. Parametric study is subsequently carried out to find out effects of different parameters on the overall performance of the density graded foam.

6.1. EFFECT OF IMPACT VELOCITY

The effect of impact velocity on density gradient structure is first investigated based on the simplified blast loading condition with the triangular velocity at the fixed duration of 0.6 ms. Figure 7(a) gives the nominal stress vs. nominal strain curves with different velocities on the impact side. It is seen that the initial peak stress and crushing stress both increases with the impact velocity, the input energy density thus rises. Furthermore, the foam deformation subjected to high velocity impact ceased at a larger strain while it was crushed with smaller deformation under a lower velocity impact. One of the explanations is that when the impact velocity is sufficiently high in the progressive failure mode, cell walls crushing occurs on the top surface with the crushing band moving down toward to the bottom constrained plate in a nearly uniform manner (Figure 5(c)), hence the crushing band propagates with a long time due to the inertia effect so that the foam is compacted with larger displacement.

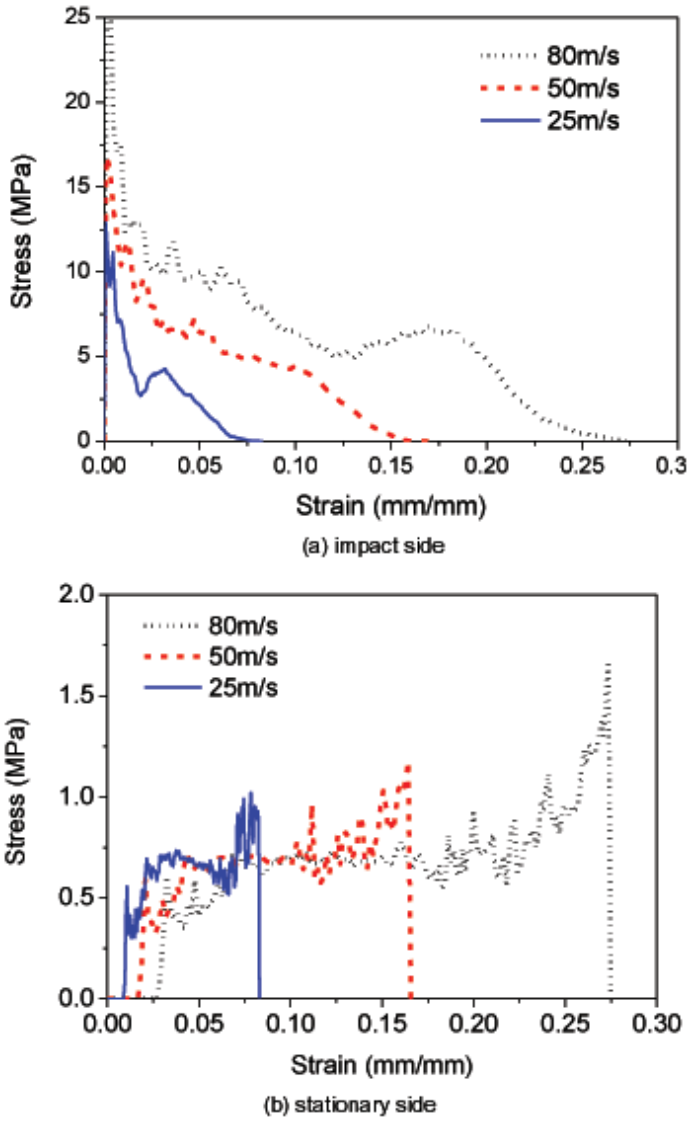

Figure 7: Effect of impact velocity on compressive stress vs. nominal strain.

It is also interesting to see that the nominal stress at the stationary side under dynamic compression is so different from that at the moving side, as shown in Figure 7(b). Although the energy density at the bottom increases with the impact velocity, the plateau stresses are approximately the same over small strain range at the stationary side, which means that the force transferred to the substrate can be constantly low at a desirable value.

The efficiency of energy absorption is subsequently discussed when the foam materials are applied different impact velocities based on the same loading duration. As can be seen from Figure 8, the graded foam owns an apparent advantage that its energy absorbing efficiency factor always outweigh the other foam core compositions' whatever the velocity

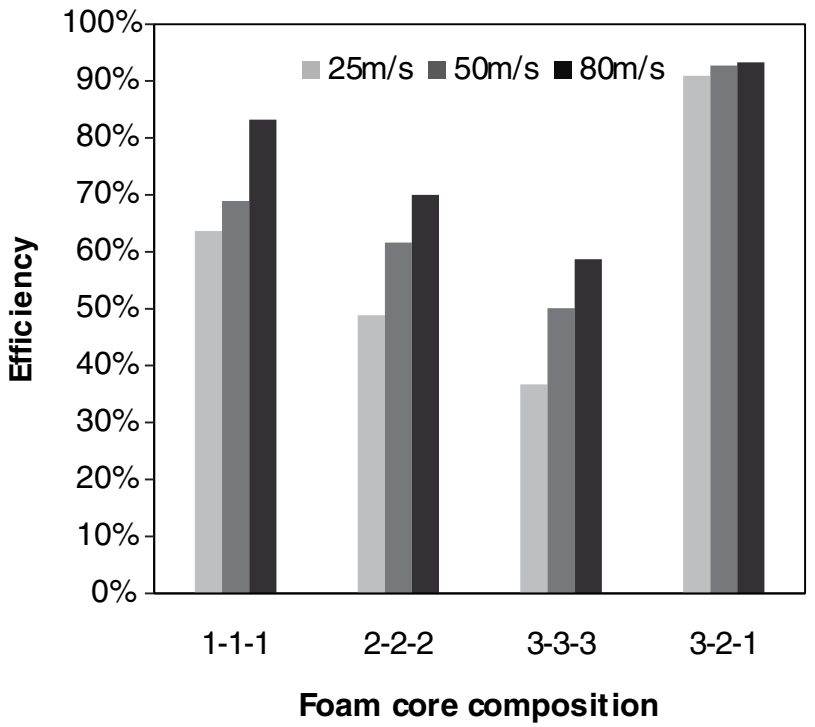

Figure 8: Effect of impact velocity on energy absorption efficiency.

is, and the energy absorbing efficiency improves by increasing the magnitude of velocity. However, this rising tendency is more obvious for materials with uniform densities, while only slight increment is observed for the foam core with density gradient.

In summary, the impact velocity hardly influence the density gradient foam's transmitted stress, which is proved to be much lower than the stress at stationary side of the homogenous foam core composition. There is also little effect of velocity on the relatively high energy absorption efficiency of graded structure, even though it substantially increases the absorbing efficiency of the homogenous foams. Therefore, under various velocity impact conditions, it would be beneficial to utilize the energy absorbing capability of the graded aluminium foam when it is necessary to reduce the peak impact load transferred to the structure under protection and obtain the energy absorption efficiency at a steadily high state.

6.2. EFFECT OF APPLIED LOAD DURATION

Five cases with varying durations are investigated in this subject of ongoing study, the initial impact velocity of the triangular loading condition is maintained as 80 m/s, the size is set up as 50×50 mm for all samples and triangular load of impact is employed.

Figure 9 shows the curves of nominal stress-strain both at the impact side and stationary side when the density graded material is subjected to the dynamic load. Increasing the duration of the applied load increases the overall deformation of the foam; nonetheless, the density graded foam will continue to be fully densified, provided that the impact duration reaches a certain value. For those totally compacted foams, the nominal strain ε_n is determined at the overall displacement of 25 mm (i.e. 50% deformation of the foam) in the below comparisons.

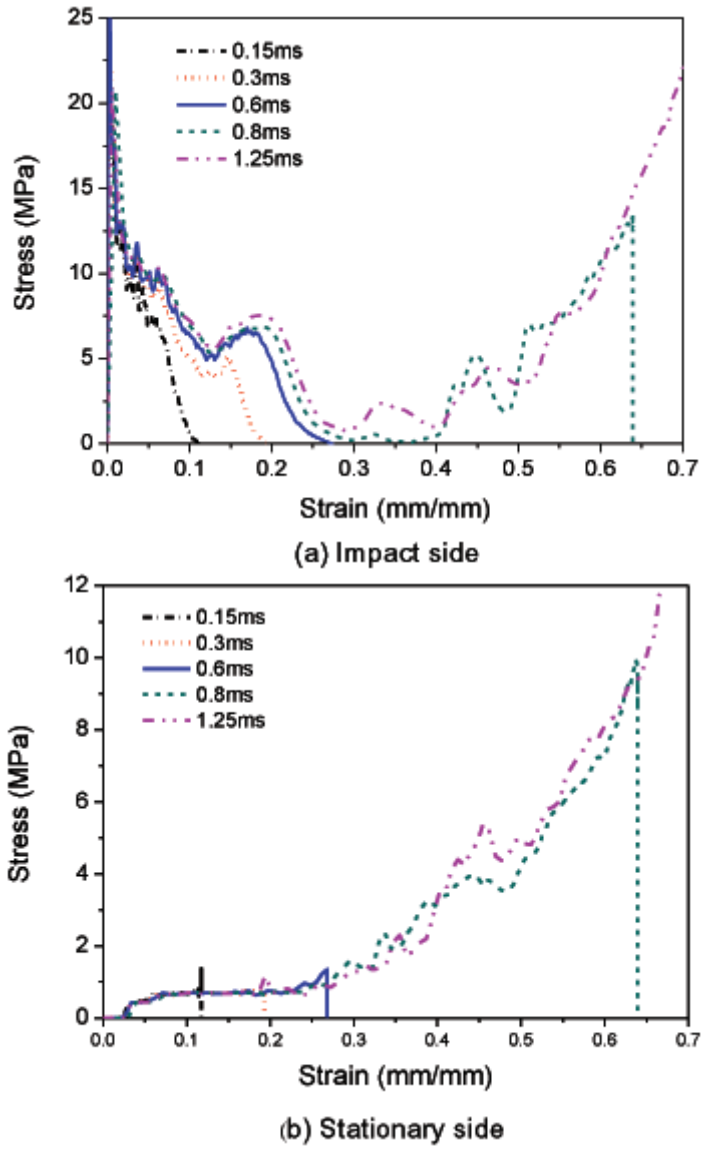

Figure 9: Effect of impact duration on compressive stress vs. nominal strain.

In terms of the energy absorption capacity, the absorbed energy rises with the increase of applied load duration at the impact side as well as the incremental amount of transferred energy showed at the stationary side. Especially after the critical duration of 0.6 ms, which can be approximately predicted in the process by determining the reflected overpressure in CONWEP [24] functions, the capacity of energy absorption per volume is immensely increased at the impact side but more residual energy is possibly transmitted to the protected structure simultaneously.

The data shown in Figure 10 illustrates the effect of applied load duration on the energy absorption efficiency. It is noted that the superiority of density gradient material also exists

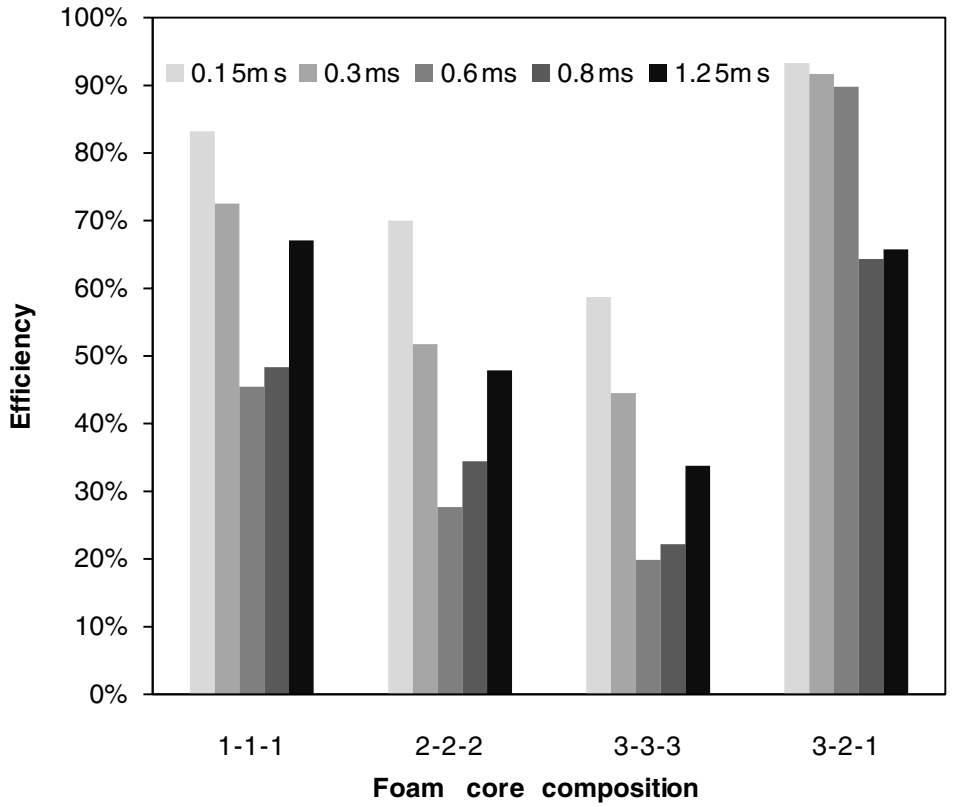

Figure 10: Effect of impact duration on energy absorption efficiency.

as it is more efficient at mitigating the blast load compared with other uniform-density foam cores under disparate impact durations. Specifically, the absorption efficiency of the foams with uniform density dramatically drops from the peak to the lowest point when the duration is varied from 0.15 ms to 0.6 ms, but it increases over the crucial duration. The dramatic turning point is also observed for graded foam at 0.8 ms; however, its energy absorbing efficiency almost keeps consistently low after the full compression.

Consequently, the effect of impact duration is distinct in that it will increase the volumetric energy absorption capacity of gradient aluminium material at the impact side but decrease the absorbing efficiency by increasing the duration.

6.3. EFFECT OF SAMPLE THICKNESS

It is also seen from Figure 9(b) that the compressive stress at the stationary side is held relatively low with the impact load duration less than 0.6 ms when the size of graded foam is kept 50×50 mm. Therefore, in order to control the transmitted stress not to exceed the desirable low value if the structure sustains load over the critical duration of 0.6 ms, it is necessary to increase the foam thickness in the following study to take full advantage of the graded foam.

The effect of thickness is investigated with the specimen size at the range of 80×80 mm, 100×100 mm and 120×120 mm, which are composed of the same density ratios (i.e. 11.1%, 14.8 and 18% relative densities). In the FE simulation, the sample size is expanded by

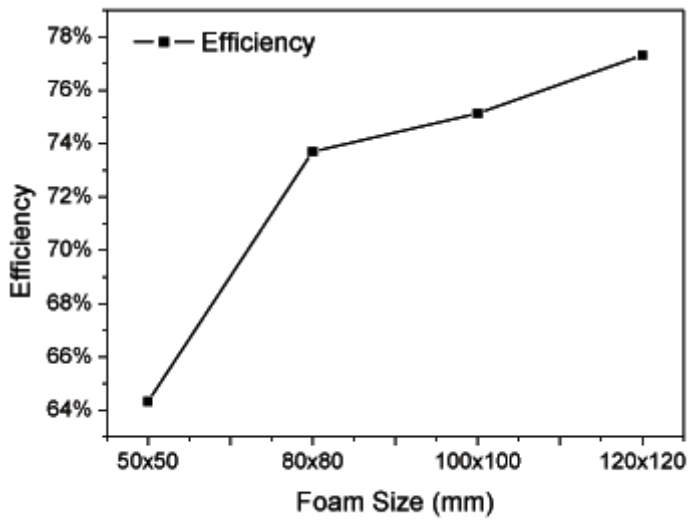

(a) Energy absorbtion efficiency

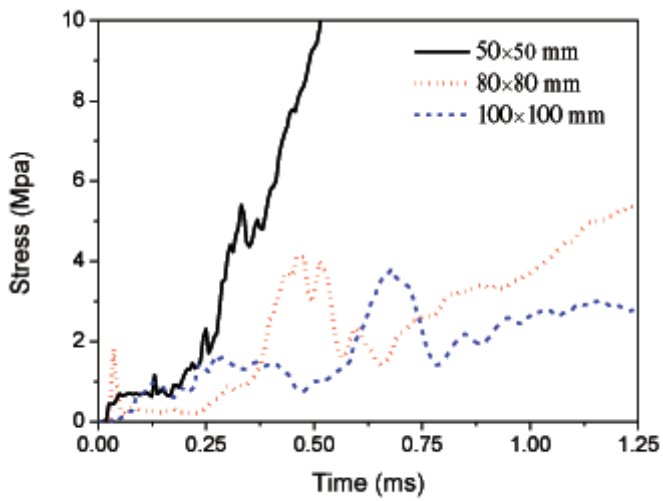

(b) Compressive stress vs. time at stationary side

Figure 11: Effect of sample thickness.

generating more cells in the larger domain, but the individual cell size does not change in the corresponding foam layer. The comparison of energy absorbing efficiency is firstly carried out based on the same initial impact velocity of 80 m/s and the fixed impact loading duration of 0.8 ms. The results in Figure 11(a) suggest that increasing the thickness of sample can augment the energy absorption efficiency, in other words, the residual energy sustained by the protected structure will be substantially reduced if the foam layer is sufficiently thick.

Figure 11(b) then gives the nominal stress time histories of different samples at the stationary side with the same impact velocity of 80 m/s and load duration of 1.25 ms. It is apparently seen that the graded foam with size of 80×80 mm is gradually compacted in a long time whilst the previous simulation of 50×50 mm specimen was completely compressed at a

larger plastic strain (Figure 9(b)) with a much steeper rising slope in a short time. The crushing stress of the sample with a larger size of 100×100 mm increases to a certain point then drops to a constant value over the later impact duration, which means that the compression behaviour of the specimen is ceased before it is fully densified. Since it is discussed above that the energy absorption efficiency is higher before the critical load duration causing full crushing, the largest density graded foam shows the optimal results in the efficiency.

7. CONCLUSION

In the FE simulations, several samples with different relative densities have been numerically simulated using ANSYS/LS-DYNA to calibrate the results with experimental tests. The numerically simulated nominal stress vs. strain curves of the aluminium foam at low strain rates agree well with the laboratory results of CYMAT material conducted by Ruan *et al* [9].

From the numerical modelling point of view, the energy absorption capability is sensitive to its relative density that the energy absorbing capacity can be enhanced by boosting the relative density of foam; however, it lowers the efficiency of absorption. Accordingly, the density graded aluminium, which has the most efficient energy absorbing performance and greater absorption capacity among other homogenous foam combinations, is studied in detail.

The parametric studies indicate that the effect of impact velocity on the volumetric energy absorption of the graded aluminium material is notable that the initial peak stress and crushing stress at impact side both increase with an increment of impact velocity, whereas the transmitted stress remains to be low in spite of the velocity variation. The velocity effect is almost negligible on graded structure's high energy absorption efficiency compared with the enormous change on a homogenous one. In terms of the analysis of the impact duration effect, it is interesting to find that the absorbing efficiency can be reduced by increasing the applied load duration, on the contrary, the energy absorption capacity improves, and one critical duration results in the substantial alteration is noted. Therefore, the study on effect of specimen thickness is conducted in case the blast load applied to the density gradient structure is over the critical duration. The results demonstrate that the thicker the specimen, the higher energy absorbing efficiency the material has

ACKNOWLEDGEMENTS

The authors would like to acknowledge the support of the Collaborative Research Fund with Overseas, Hong Kong and Macau Scholars (grant number 51028801) of the National Natural Science Foundation of China.

REFERENCES

[1] Lu G, Yu TX, Energy absorption of structures and materials, Cambridge: Woodhead Publishing Ltd., 2003.

[2] Gibson LJ, Ashby MF, Cellular solids: Structure and properties, Cambridge University Press, (1997).

[3] Ashby MF, Evans AG, Fleck NA, Gibson LJ, Hutchinson JW, Wadley HNG, Metal Foams: A Design Guide in, Butterworth-Heinemann, 2000.

[4] Shu DW, Goh JH, Modelling of Young's modulus of foams, Plastics Rubber and Composites, 30 (2001) 461–467.

[5] Andrews E, Sanders W, Gibson LJ, Compressive and tensile behaviour of aluminum foams, Materials Science and Engineering a-Structural Materials Properties Microstructure and Processing, 270 (1999) 113–124.

[6] Paul A, Ramamurty U, Strain rate sensitivity of a closed-cell aluminum foam, Materials Science and Engineering a-Structural Materials Properties Microstructure and Processing, 281 (2000) 1–7.

[7] Wang ZH, Shen JH, Lu GX, Zhao LM, Compressive behavior of closed-cell aluminum alloy foams at medium strain rates, Materials Science and Engineering a-Structural Materials Properties Microstructure and

Processing, 528 (2011) 2326–2330.

[8] Mukai T, Kanahashi H, Miyoshi T, Mabuchi M, Nieh TG, Higashi K, Experimental study of energy absorption in a close-celled aluminum foam under dynamic loading, Scripta Materialia, 40 (1999) 921–927.

[9] Ruan D, Lu G, Chen FL, Siores E, Compressive behaviour of aluminium foams at low and medium strain rates, Composite Structures, 57 (2002) 331–336.

[10] Overaker DW, Cuitino AM, Langrana NA, Effects of morphology and orientation on the behavior of two-dimensional hexagonal foams and application in a re-entrant foam anchor model, Mechanics of Materials, 29 (1998) 43–52.

[11] Silva MJ, Gibson LJ, The effects of non-periodic microstructure and defects on the compressive strength of two-dimensional cellular solids, International Journal of Mechanical Sciences, 39 (1997) 549–563.

[12] Zheng ZJ, Yu JL, Li JR, Dynamic crushing of 2D cellular structures: A finite element study, International Journal of Impact Engineering, 32 (2005) 650–664.

[13] Papka SD, Kyriakides S, Experiments and full-scale numerical simulations of in-plane crushing of a honeycomb, Acta Materialia, 46 (1998) 2765–2776.

[14] Zhu F, Zhao LM, Lu GX, Gad E, A numerical simulation of the blast impact of square metallic sandwich panels, International Journal of Impact Engineering, 36 (2009) 687–699.

[15] Daxner T, Rammerstorfer FG, Bohm HJ, Adaptation of density distributions for optimising aluminium foam structures, Materials Science and Technology, 16 (2000) 935–939.

[16] Ajdari A, Canavan P, Nayeb-Hashemi H, Warner G, Mechanical properties of functionally graded 2-D cellular structures: A finite element simulation, Materials Science and Engineering a-Structural Materials Properties Microstructure and Processing, 499 (2009) 434–439.

[17] Lee SJ, Wang JQ, Sankar BV, A micromechanical model for predicting the fracture toughness of functionally graded foams, International Journal of Solids and Structures, 44 (2007) 4053–4067.

[18] Meguid SA, Cheon SS, El-Abbasi N, FE modelling of deformation localization in metallic foams, Finite Elements in Analysis and Design, 38 (2002) 631–643.

[19] Zhu HX, Thorpe SM, Windle AH, The geometrical properties of irregular two-dimensional Voronoi tessellations, Philosophical Magazine a-Physics of Condensed Matter Structure Defects and Mechanical Properties, 81 (2001) 2765–2783.

[20] Luxner MH, Stampfl J, Pettermann HE, Numerical simulations of 3D open cell structures - influence of structural irregularities on elasto-plasticity and deformation localization, International Journal of Solids and Structures, 44 (2007) 2990–3003.

[21] Li QM, Maharaj RN, Reid SR, Penetration resistance of aluminium foam, International Journal of Vehicle Design, 37 (2005) 175–184.

[22] Ruan D, Lu G, Wang B, Yu TX, In-plane dynamic crushing of honeycombs - a finite element study, International Journal of Impact Engineering, 28 (2003) 161–182.

[23] Ma GW, Ye ZQ, Shao ZS, Modeling loading rate effect on crushing stress of metallic cellular materials, International Journal of Impact Engineering, 36 (2009) 775–782.

[24] CONWEP, Technical Manual TM5-855-1, Fundamentals of Protective Design for Conventional Weapons, US Department of the Army,Washington, DC, 1986.